

Journal of Materials Chemistry C

Accepted Manuscript



This is an *Accepted Manuscript*, which has been through the Royal Society of Chemistry peer review process and has been accepted for publication.

Accepted Manuscripts are published online shortly after acceptance, before technical editing, formatting and proof reading. Using this free service, authors can make their results available to the community, in citable form, before we publish the edited article. We will replace this *Accepted Manuscript* with the edited and formatted *Advance Article* as soon as it is available.

You can find more information about *Accepted Manuscripts* in the [Information for Authors](#).

Please note that technical editing may introduce minor changes to the text and/or graphics, which may alter content. The journal's standard [Terms & Conditions](#) and the [Ethical guidelines](#) still apply. In no event shall the Royal Society of Chemistry be held responsible for any errors or omissions in this *Accepted Manuscript* or any consequences arising from the use of any information it contains.

Silver Nanoparticles Deposited on TiO₂-Coated Cicada and Butterfly Wings as Naturally Inspired SERS Substrates

Ichiro Tanahashi^{*a}, Yoshiyuki Harada^a

^aNanomaterials and Microdevices Research Center, Osaka Institute of Technology, 5-16-1 Omiya, Asahi-ku, Osaka, 535-8585, Japan

ichiro.tanahashi@oit.ac.jp, yoshiyuki.harada@oit.ac.jp

Abstract Ag nanoparticles were photocatalytically deposited on TiO₂-coated cicada and butterfly wings (Ag/TiO₂-coated wings). Wings of two species of cicadas (*Cryptotympana facialis* and *Graptopsaltria nigrofuscata*) and one species of butterfly (*Parnassius citrinarius*) were investigated as substrates based on natural materials. Uniform ordered nanopillar array and irregular sub-micron sized pillar structures were observed on the wing surfaces of *Cryptotympana facialis* and *Graptopsaltria nigrofuscata*, respectively. On the surface of wing scales of *Parnassius citrinarius*, uniform ordered ridge structure was observed. A small number of Ag nanoparticles were also deposited on the intact bare cicada and butterfly wings without TiO₂ (Ag/wings) by the photoreduction. The surface enhanced Raman scattering (SERS) signal intensities of Rhodamine 6G (R6G) dripped and dried on the Ag thin film sputtered on glass slides, Ag/wings and Ag/TiO₂-coated wings increased in that order. In particular, the SERS signal intensities of R6G on the Ag/TiO₂-coated wing of *Cryptotympana facialis* were more than 25 times larger than those on the Ag thin film.

1 Introduction

The synthesis of metal nanoparticles is of current interest due to their interesting optical, electrical and thermal properties as compared with the bulk metal. The metal nanoparticles have been applied in fields such as electronics,^{1,2} photonics,^{3,4} catalysis⁵ and surface-enhanced Raman scattering (SERS).⁶⁻⁹ In particular, SERS technique was shown to be a very effective analytical tool for the detection of trace amount of chemical and biological agents. As the SERS-active materials, metal films with a rough surface morphology and metal nanoparticles have been investigated.^{10,11} In the case of metal nanoparticles, the local electromagnetic field enhancement induced by the excitation of the localized surface plasmon resonance (LSPR) is the major mechanism for SERS. It is reported that the local electromagnetic field enhancement increases with increasing the size of metal particles.¹² On the other hand, the absorption of light become smaller and the light scattering become larger with increasing the size of the metal particles.¹² Therefore, it is essential to ascertain the optimal size of the metal nanoparticles to realize the maximum SERS intensity. However, there are few studies on the SERS properties of the metal nanoparticles with more than 100 nm in diameter.¹³ It has been also reported that the LSPR properties are strongly dependent on the size and shape of the metal nanoparticles.^{14,15} In particular, silver (Ag) nanoparticles with clear LSPR absorption in the visible wavelength region are the most suitable candidate for SERS substrates. However, the size control is still one of the challenging problems.

It is known that the SERS properties of the deposited metal nanoparticles on the base substrates are affected by the surface nanostructures of them. As the base substrates, the artificial ones such as glasses, plastics, ceramics and semiconductors are widely used. On the other hand, some biological surfaces of insect wings are structured at the micro/nanometer scale and have a lot of functional properties such as antireflection,¹⁶ photonic bandgap¹⁷ and superhydrophobicity.¹⁸ By using the micro/nanostructured surfaces of natural biological materials, scientists have been tried to develop new types of SERS substrates.^{16,19-23} The Ag replicas of butterfly scales as SERS substrates have been studied.¹⁹⁻²² However, a three-step complicated process was needed in order to produce the Ag replicas with three dimensional submicrostructures from biological templates.²⁰ To make SERS technique as a general analytical tool, the fabrication of the SERS substrates should become much cheaper and more easily handled. Besides the butterfly scales, it is observed that the uniform ordered nanopillar array structures on some species of cicada wing surfaces. In our previous studies,^{24,25} we have reported that the preparation, SPR-sensing and SERS properties of the Ag nanoparticles which were photocatalytically deposited on glass slides, intact bare cicada wings and TiO₂-coated cicada wings with nanopillar array structures. Strong SERS signals of Rhodamine 6G adsorbed on the Ag nanoparticles deposited onto TiO₂-coated cicada wings were clearly observed.²⁵ However, it is not clear what types of micro/nanostructured surfaces of insect wings are suitable for naturally inspired SERS substrates.

In this paper, on the basis of the SERS properties of the Ag thin film sputtered on glass slides, we have compared those of the Ag nanoparticles deposited on TiO₂-coated and TiO₂-uncoated wings of three types of insects (two species of cicadas and one species of butterfly) with different micro/nanostructured surfaces.

2 Experimental details

2.1 Material (Animals)

The cicadas and butterflies were captured respectively in Osaka prefecture and Shiga prefecture in the Kansai region (Honshu) of Japan. Wing samples of cicadas and butterflies were collected from *Cryptotympana facialis* (a black cicada with clear and transparent wings), *Graptopsaltria nigrofuscata* (a black cicada with brown wings) and *Parnassius citrinarius* (the Parnassiinae butterfly, white and subhyaline markings on the forewings). These two species of cicadas are common in the Kansai region of Japan. In this experiment, the dorsal forewings of male cicada and butterfly were used. The forewings were cut off from the body at the base with fine scissors. Before the dip-coating process, the forewings (45-55 mm in length) of individual cicada were rinsed using ethyl alcohol and deionized water to remove contaminant and dried at room temperature. On the other hand, the forewings (about 30 mm in forewing-length) of butterfly were used without any treatment.

2.2 Preparation of Ag/TiO₂-coated wings, Ag/wings and Ag thin film

The preparation processes of the Ag nanoparticles deposited on TiO₂-coated cicada and butterfly wings (Ag/TiO₂-coated wings) and Ag nanoparticles deposited directly on TiO₂-uncoated intact bare cicada and butterfly wings (Ag/wings) have been described previously.²⁵ TiO₂ was coated on both sides of the forewings of the cicada and butterfly from anatase sol (Ishihara Sangyo Kaisha, ST-K211, crystallite size of about 3 nm) by using a dip-coating technique. The TiO₂-coated wings were dried at 70°C for 10 min. The resulting wings were soaked in a mixture of 2 mL of a 5.0×10^{-2} mol L⁻¹ AgNO₃ aqueous solution and 4 mL of ethyl alcohol (1.67×10^{-2} mol L⁻¹ of Ag⁺ ions) in a petri dish (5 cm in diameter) about 10 mm away under an UV lamp. The lamp used was a 15 W low-pressure mercury lamp (a germicidal lamp, 253.7 nm) and the wings were irradiated with a power density of about 1 mWcm⁻² for 2 h. In the case of the preparation of the Ag/TiO₂-uncoated wings (Ag/wings), forewings of the insects without TiO₂ were also irradiated with UV light as the above mentioned procedure. The resultant Ag/TiO₂-coated wings and Ag/wings were washed with deionized water, finally dried in air. The samples were kept in a vacuum desiccator. All the preparation procedures of the Ag nanoparticle deposition were carried out at room temperature. All compounds were of reagent grade and were used without further purification. Aqueous solutions of AgNO₃ were prepared using deionized water (more than 1 MΩ cm). As a reference, Ag thin films were prepared by an RF magnetron sputtering system. The Ag (99.9%, 2 inch in diameter) target was used. The substrate used was a glass slide and it was not intentionally heated. Sputtering was carried out in Ar gas of about 2 Pa and the typical applied RF power of the Ag target was 50 W.

2.3 Characterization of Ag/TiO₂-coated wings, Ag/wings and intact bare wings,

Digital photographs of the Ag/TiO₂-coated wings, Ag/wings and insect specimens were taken using a digital camera (Fujifilm Corporation). Surface morphologies of the Ag/TiO₂-coated wings, Ag/wings and intact bare cicada and butterfly were examined by scanning electron microscopy

(SEM) using a VE-8800 scanning electron microscope (Keyence Corporation) at an acceleration voltage of 12 kV and a working distance of about 11 mm.

X-ray diffraction (XRD) measurements were carried out on a RINT 2000 X-ray diffractometer (Rigaku Corporation), using Cu K α radiation working at 40 kV and 40 mA. The crystallite sizes, d , of the Ag/TiO₂-coated wings, Ag/wings and TiO₂ (ST-K211) powders were estimated using the Scherrer equation: $d = 0.9\lambda / \beta \cos \theta$, where λ is the wavelength of X-ray source (0.154059 nm) and β the full width at half maximum (FWHM) of the X-ray diffraction peak at the diffraction angle θ . The absorption spectra were measured from 200 to 800 nm on an UV-3100PC dual beam spectrophotometer (Shimadzu Corporation).

2.4 SERS spectra measurements of Ag/TiO₂-coated wings, Ag/wings and Ag thin film

SERS spectra measurements were performed by irradiating the samples with 50 mW of 514.5 nm line of Ar⁺ laser in back scattering geometry at room temperature. A 50 \times long distance objective and a cooled CCD detector were employed. The laser beam was focused on a spot with a diameter of approximately 2 μ m and the data acquisition time for each measurement was 1 s. The intensities of Raman spectra of 10⁻³ and 10⁻⁶ mol L⁻¹ Rhodamine 6G (R6G, 2 μ L) dripped and dried on the Ag/TiO₂-coated wings and Ag/wings at near the center of the dorsal forewings were compared. As a reference, 10⁻³ mol L⁻¹ of R6G (2 μ L) dripped and dried on the Ag thin films sputtered on glass slides were prepared.

3 Results and Discussion

3.1 Digital photographs and SEM images of the Ag/TiO₂-coated wings, Ag/wings and intact bare insect wings

We have chosen three types of cicada and butterfly wings with significant differences in micro/nanostructures shown in Fig. 1. The wing colors of *Cryptotympana facialis* (a-1 in Fig. 1) and *Graptosaltria nigrofuscata* (b-1) are transparent and brown, respectively. In the SEM micrograph of *Cryptotympana facialis* (a-2), a dense nanopillar array structure is seen. Diameters and separations of the nanopillar array are about 130 nm and 30-130 nm, respectively. The morphology of the surface structures was almost the same for the dorsal and ventral surfaces. It is known that the nanopillar array structures have an important role to play in the antireflection properties of the wings.¹⁶ On the other hand, the irregular shaped pillars of sub-micron sizes are seen on the wing of *Graptosaltria nigrofuscata* shown in the SEM micrograph (b-2). In the figure, some of the pillars seem to be connected with each other. The forewing color of *Parnassius citrinarius* is white and subhyaline markings (c-1) and the uniform ordered ridge structure is observed on the surface of the wing scales of both white and subhyaline markings of the wings shown in the SEM micrograph (c-2).

In all the investigated Ag/TiO₂-coated cicada and butterfly wings, the colors of the wings were changed to metallic gray after the photoreduction of Ag⁺ ions onto TiO₂-coated wings. These color changes indicate the formation of Ag metal on the TiO₂-coated wings. This is due to that the TiO₂ coated on the wings works as a photocatalyst. It is suggested that the photo-generated electrons from

the TiO₂ photocatalyst reduced Ag⁺ ions to Ag metal effectively. On the other hand, in the case of the Ag/wings, the color of the wings was changed to dark brown.

Figure 2 shows typical SEM images of the Ag/TiO₂-coated wings and Ag/wings of *Cryptotympana facialis*, *Graptopsaltria nigrofuscata* and *Parnassius citrinarius*. In the case of Ag/TiO₂-coated wing of *Cryptotympana facialis* shown in Fig. 2 (a-3), densely stacked Ag nanoparticles with 100-250 nm in diameter are seen on the nanopillar array structure. A part of the micrograph field including 150 particles was randomly selected to analyze the size distribution. The average diameter of the Ag nanoparticles was estimated to be 165 nm with a standard deviation of 50 nm. On the other hand, in the case of the Ag/wing of *Cryptotympana facialis*, a part of the surface is covered with Ag nanoparticles and Ag films as shown in Fig. 2 (a-4). In this case, Ag⁺ ions seem to be photoreduced inefficiently on the functional groups of chitin of the wings and by the aqueous solution of ethyl alcohol.²⁶ The nanopillar array structure of *Cryptotympana facialis* could not be covered uniformly by Ag nanoparticles. Typical SEM images of the Ag/TiO₂-coated wing and Ag/wing of *Graptopsaltria nigrofuscata* are shown in Fig. 2 (b-3) and (b-4), respectively. It is observed that the Ag nanoparticles are deposited on both parts of the nanopillars and membrane of the Ag/TiO₂-coated wing (b-3). The number of Ag nanoparticles deposited on the TiO₂-coated wing (b-3) was larger than that of the Ag/wing (b-4). In both figures, the sizes of the Ag nanoparticles were less than about 100 nm in diameter. Typical SEM images of the Ag/TiO₂-coated wing and Ag/wing of *Parnassius citrinarius* are shown in Fig. 2 (c-3) and (c-4), respectively. The uniform ordered ridge structure of the Ag/TiO₂-coated forewing are covered with the Ag films and Ag nanoparticles shown in Fig. 2 (c-3). The grooves of the ridge structure were filled up with Ag. On the other hand, in the case of the Ag/wing, a small part of the surface of the ridge structure is covered with various sizes of the Ag particles (c-4). Among the investigated TiO₂-coated and TiO₂-uncoated cicada and butterfly wings, the densely stacked Ag nanoparticles with 165 nm in average diameter were observed only on the TiO₂-coated three dimensional nanopillar array structures of the wings of *Cryptotympana facialis*.

In the case the Ag thin film sputtered on glass slides, the mirror-like surface of the film was smooth and the characteristic structures were not seen by the SEM observation.

3.2 XRD patterns of the Ag/TiO₂-coated wings and Ag thin film

Figure 3 shows the XRD patterns of the Ag/TiO₂-coated wings of (a) *Cryptotympana facialis*, (b) *Graptopsaltria nigrofuscata*, (c) *Parnassius citrinarius* and that of (d) the Ag thin film. In the figure, all the spectra show the peak at $2\theta = 38.1^\circ$ which was assigned to the (111) reflection line of cubic Ag. In the patterns of Fig. 3 (a) and (d), in addition to the peak at $2\theta = 38.1^\circ$, the peak at $2\theta = 44.3^\circ$ assigned to the (200) reflection line of cubic Ag is observed. The (111) reflection line peak intensities of the Ag/TiO₂-coated wings of (c), (b) and (a) increased in that order. From this result, it is suggested that the amount of deposited Ag of the Ag/TiO₂-coated wing of (a) *Cryptotympana facialis* is larger than those of the Ag/TiO₂-coated wings of (b) *Graptopsaltria nigrofuscata* and (c) *Parnassius citrinarius*. The crystallite sizes of Ag were calculated to be 22-29 nm from the (111) reflection peak broadening of all the samples shown in Fig. 3. Therefore, the deposited Ag on the

Ag/TiO₂-coated wings and the Ag thin film prepared by the sputtering were consisting of small Ag crystallites and the crystallite sizes of them were almost the same.

3.3 UV-Vis absorption spectra of the Ag/TiO₂-coated wings, Ag/wings and insect bare wings

Figure 4 (a) shows the optical absorption spectra of (a- I) Ag/TiO₂-coated wing, (a- II) Ag/wing and (a-III) intact bare wing of *Cryptotympana facialis*. In the figure, the spectra (a- II) and (a-III) show a clear absorption peak at about 277 nm attributed to the nanopillar array structure of the bare cicada wings.¹⁶ The spectra (a- I) and (a- II) show the broad LSPR absorption bands of the Ag nanoparticles around 445 nm and around 430 nm, respectively. The broad absorption bands of both spectra suggested that the size distribution and shape variation of the Ag nanoparticles were large. The absorbance of the LSPR of the spectrum (a- I) at 445 nm was about twice as large as that of the spectrum (a- II), indicating that the deposited amount of Ag nanoparticles of the Ag/TiO₂-coated wing was larger than that of the Ag/wing. In the spectra (a- I) and (a- II), the large background absorptions are observed. These are probably due to the light scattering of the Ag/TiO₂-coated wing and Ag/wing. Figure 4 (b) shows the optical absorption spectra of (b- I) Ag/TiO₂-coated wing, (b- II) Ag/wing and (b-III) intact bare wing of *Graptosaltria nigrofuscata*. In the spectrum (b-III), the absorption from 300 to 800 nm with a peak at 713 nm is observed and it is probably due to the brown color pigments of the intact bare wing of *Graptosaltria nigrofuscata*. The absorbance of the spectrum (b- I) was larger than that of the spectrum (b- II) in all the investigated wavelength range, indicating the deposited amount of Ag of the Ag/TiO₂-coated wing was larger than that of the Ag/wing. In the case of *Graptosaltria nigrofuscata*, the weak LSPR absorption was observed around 490 nm in the spectrum (b- II). Because of the large background absorption, the LSPR absorption could not be observed in the spectrum (b- I). The optical absorption spectra of (c- I) Ag/TiO₂-coated wing, (c- II) Ag/wing and (c-III) intact bare wing of *Parnassius citrinarius* are shown in Figure 4 (c). In these spectra, only the spectrum (c- I) shows the weak and broad LSPR absorption band around 360 nm and the absorbance of the spectrum (c- I) in all the investigated wavelength range is larger in comparison with those of the spectra (c- II) and (c-III).

Among the investigated optical absorption spectra of the Ag/TiO₂-coated wing, Ag/wing and intact bare wing of insects, the spectra of the Ag/TiO₂-coated wing and Ag/wing of *Cryptotympana facialis* showed the clear LSPR absorption of Ag nanoparticles.

3.4 SERS spectra of R6G adsorbed on the Ag/TiO₂-coated wings, Ag/wings and Ag thin film

SERS spectra of R6G (10^{-3} mol L⁻¹, 2 μ L) dripped and dried on the Ag/TiO₂-coated wings of (a) *Cryptotympana facialis*, (b) *Graptosaltria nigrofuscata* and (c) *Parnassius citrinarius* are shown in Figure 5. The SERS spectrum of R6G (10^{-3} mol L⁻¹, 2 μ L) dripped and dried on (d) the Ag thin film sputtered on glass slides is also shown in the figure. The inset is the SERS spectrum of R6G (10^{-6} mol L⁻¹, 2 μ L) dripped and dried on the Ag/TiO₂-coated wing of *Cryptotympana facialis* in the wavenumber range of 1600-1700 cm⁻¹. In all the spectra (a), (b), (c) and (d) shown in Fig. 5, the observed Raman bands are assigned to R6G characteristic bands of C-H out-of-plane bend mode at ca. 774 cm⁻¹, C-H in-plane bend mode at ca. 1129 cm⁻¹, C-C stretching modes at ca. 1358, 1505 and

1649 cm^{-1} .^{27,28} The SERS signal intensities of R6G on the Ag/TiO₂-coated wings of (c) *Parnassius citrinarius* (b) *Graptosaltria nigrofuscata* and (a) *Cryptotympana facialis* increased in that order. From the inset of Fig. 5, the sensitivity of the Ag/TiO₂-coated wing of *Cryptotympana facialis* for R6G was found to be 10⁻⁶ mol L⁻¹.

Due to the differences in the coated areas of R6G between the samples (50-80 mm²), the peak intensities were normalized by the coated areas of R6G. The normalized peak intensities of R6G at 1649 cm^{-1} of the Ag/TiO₂-coated wings of (I) *Cryptotympana facialis*, (II) *Graptosaltria nigrofuscata*, (III) *Parnassius citrinarius*; the Ag/wings of (IV) *Cryptotympana facialis*, (V) *Graptosaltria nigrofuscata* and (VI) *Parnassius citrinarius* are shown in Figure 6. The normalized peak intensity of R6G at 1649 cm^{-1} of (VII) the Ag thin film sputtered on glass slides is also shown in the figure. The normalized peak intensities of R6G at 1649 cm^{-1} of the Ag/TiO₂-coated wings (I), (II), (III) and (IV) were respectively 25.4, 5.0, 2.6 and 2.0 times larger than that of (VII). On the other hand, the normalized peak intensities of R6G on the Ag/wings of (V) and (VI) were comparable to that of (VII).

From the results of SEM and XRD of the Ag/TiO₂-coated wings of *Cryptotympana facialis*, densely stacked Ag nanoparticles with an average diameter of 165 nm were observed. It seems that the Ag nanoparticles with 100-250 nm in diameter are effectively deposited on the TiO₂-coated nanopillar array structure with a pillar diameter of about 130 nm and separations of 30-130 nm. On the other hand, the Ag/TiO₂-coated wings of *Graptosaltria nigrofuscata* and *Parnassius citrinarius*, densely stacked Ag nanoparticles with diameters greater than 100 nm were not deposited. Thus, the irregular shaped pillar structure of sub-micron sizes of the wings of *Graptosaltria nigrofuscata* and the ridge structure of the wings of *Parnassius citrinarius* were not suitable structures to obtain the Ag nanoparticles with more than 100 nm in diameter.

The SERS signal intensities of R6G adsorbed on the Ag thin films, Ag/wings and Ag/TiO₂-coated wings increased in that order. The TiO₂ photocatalyst coated on the cicada and butterfly wings played a significant role to deposit the Ag nanoparticles on the wings effectively by the photoreduction of Ag⁺ ions. Among the investigated cicada and butterfly wings, the self-assembled natural nanopillar array structure of the wings of *Cryptotympana facialis* was suitable for preparing the densely stacked Ag nanoparticles with diameters greater than 100 nm.

4 Conclusions

By using TiO₂ as a photocatalyst, Ag nanoparticles were effectively deposited on the TiO₂-coated wings (Ag/TiO₂-coated wings) of two species of cicadas (*Cryptotympana facialis* and *Graptosaltria nigrofuscata*) and one species of butterfly (*Parnassius citrinarius*). The Ag/TiO₂-coated wings with larger-area, low-cost and high-performance were investigated as SERS substrates based on natural materials. The SERS signal intensities (514.5 nm excitation line) of R6G adsorbed on the Ag/TiO₂-coated wings were larger than those of the Ag thin film sputtered on glass slides. Among the investigated Ag/TiO₂-coated wings, densely stacked Ag nanoparticles with 165 nm in average diameter were obtained by using the three dimensional nanopillar array structures of the wings of *Cryptotympana facialis*. In the SERS spectra, the peak intensity of R6G at 1649 cm^{-1} of the

Ag/TiO₂-coated wing of *Cryptotympana facialis* was 25 times larger than that of the Ag thin film. The Ag/TiO₂-coated wings with Ag nanoparticles deposited on nanopillar array nanostructures seem to be a promising candidate for naturally inspired SERS substrates.

Acknowledgements

This work was supported in part by “Senryakuteki Kenkyuukiban Keisei Shienjigyou (industry to support private universities building up their foundations of strategic research)” Project for Private Universities: subsidy from MEXT (Ministry of Education, Culture, Sports, Science and Technology), Japan.

Figures and Table

Fig. 1. Digital photographs and SEM images of wings of insect specimens: (a-1) and (a-2) represent digital photograph and SEM image of wing of *Cryptotympana facialis*, respectively; (b-1) and (b-2) represent digital photograph and SEM image of wing of *Graptosaltria nigrofuscata*, respectively; (c-1) and (c-2) represent digital photograph and SEM image of wing of *Parnassius citrinarius*, respectively.

Fig. 2. SEM images of Ag/TiO₂-coated wings and Ag/wings: (a-3) and (a-4) represent SEM images of Ag/TiO₂-coated wing and Ag/wing of *Cryptotympana facialis*, respectively; (b-3) and (b-4) represent SEM images of Ag/TiO₂-coated wing and Ag/wing of *Graptosaltria nigrofuscata*, respectively; (c-3) and (c-4) represent SEM images of Ag/TiO₂-coated wing and Ag/wing of *Parnassius citrinarius*, respectively.

Fig. 3. X-ray diffraction patterns of Ag/TiO₂-coated wings of (a) *Cryptotympana facialis*, (b) *Graptosaltria nigrofuscata*, (c) *Parnassius citrinarius* and that of (d) Ag thin film sputtered on glass slides.

Fig. 4. Optical absorption spectra of (I) Ag/TiO₂-coated wing, (II) Ag/wing and (III) intact bare wing of (a) *Cryptotympana facialis*, those of (b) *Graptosaltria nigrofuscata* and those of (c) *Parnassius citrinarius*.

Fig. 5. SERS spectra of R6G (10^{-3} mol L⁻¹, 2 μ L) dripped and dried on Ag/TiO₂-coated wings of (a) *Cryptotympana facialis*, (b) *Graptosaltria nigrofuscata*, (c) *Parnassius citrinarius* and that of (d) Ag thin film. Inset: SERS spectrum of R6G (10^{-6} mol L⁻¹, 2 μ L) dripped and dried on Ag/TiO₂-coated wing of *Cryptotympana facialis*.

Fig. 6. Comparison of normalized 1649 cm⁻¹ SERS signal intensities of R6G (10^{-3} mol L⁻¹, 2 μ L) dripped and dried on seven types of samples: (I) Ag/TiO₂-coated wing of *Cryptotympana facialis*, (II) Ag/TiO₂-coated wing of *Graptosaltria nigrofuscata*, (III) Ag/TiO₂-coated wing of *Parnassius citrinarius*, (IV) Ag/wing of *Cryptotympana facialis*, (V) Ag/wing of *Graptosaltria nigrofuscata*, (VI) Ag/wing of *Parnassius citrinarius* and (VII) Ag thin film sputtered on glass slides.

References

- 1 W. Lu and C. M. Lieber, *Nat. Mater.*, 2007, **6**, 841-850.
- 2 T. C. Karni, R. Langer and D. S. Kohane, *ACS Nano*, 2012, **6**, 6541-6545.
- 3 Y. Shen, C. S. Friend, Y. Jiang, D. Jakubczyk, J. Swiatkiewicz and P. N. Prasad, *J. Phys. Chem. B*, 2000, **104**, 7577-7587.
- 4 I. Tanahashi, Y. Manabe, T. Tohda, S. Sasaki and A. Nakamura, *J. Appl. Phys.*, 1996, **79**, 1244-1249.
- 5 S. B. Kalidindi and B. R. Jagirdar, *ChemSusChem*, 2012, **5**, 65-75.
- 6 C. L. Haynes and R. P. V. Duyne, *J. Phys. Chem. B*, 2003, **107**, 7426-7433.
- 7 K. Hering, D. Cialla, K. Ackermann, T. Dorfer, R. Moller, H. Schneidewind, R. Matteis, W. Fritzsche, P. Rosch and J. Popp, *Anal. Bioanal. Chem.*, 2008, **390**, 113-124.
- 8 K. Kim and K. S. Shin, *Anal. Sci.*, 2011, **27**, 775-783.
- 9 A. J. Chung, Y. S. Huh and D. Erickson, *Nanoscale*, 2011, **3**, 2903-2908.
- 10 Y. Wu, B. Zhao, W. Xu, B. Li, Y. M. Jung and Y. Ozaki, *Langmuir*, 1999, **15**, 4625-4629.
- 11 W. Xie, P. Qui and C. Mao, *J. Mater. Chem.*, 2011, **21**, 5190-5202.
- 12 K. G. Stamplecoskie and J. C. Scaiano, *J. Phys. Chem. C*, 2011, **115**, 1403-1409.
- 13 R. Prucek, A. Panacek, J. Soukupova, R. Novotny and L. Kvitek, *J. Mater. Chem.*, 2011, **21**, 6416-6420.
- 14 K.-P. Charle, W. Schulze and B. Winter, *Z. Phys. D*, 1989, **12**, 471-475.
- 15 S. Link and M. A. El-Sayed, *J. Phys. Chem. B*, 1999, **103**, 8410-8426.
- 16 P. R. Stoddart, P. J. Cadusch, T. M. Boyce, R. M. Erasmus and J. D. Comins, *Nanotechnology*, 2006, **17**, 680-686.
- 17 J. Huang, X. Wang and Z. L. Wang, *Nano Lett.*, 2006, **6**, 2325-2331.
- 18 M. Sun, A. Liang, Y. Zheng, G. S. Watson and J. A. Watson, *Bioinspir. Biomim.*, 2011, **6**, 026003.
- 19 Y. Tan, J. Gu, X. Zang, W. Xu, K. Shi, L. Xu and D. Zhang, *Angew. Chem. Int. Ed.*, 2011, **50**, 8307-8311.
- 20 Y. Tan, X. Zhang, J. Gu, D. Liu, S. Zhu, H. Su, C. Feng, Q. Liu, W. M. Law, W-J Moon and D. Zhang, *Langmuir*, 2011, **27**, 11742-11746.
- 21 B. Y. Liu, W. Zhang, H. M. Lv, D. Zhang and X. Gong, *Mater. Lett.*, 2012, **74**, 43-45.
- 22 Y. Tan, J. Gu, L. Xu, X. Zang, D. Liu, W. Zhang, Q. Liu, S. Zhu, H. Su, C. Feng, G. Fan and D. Zhang, *Adv. Funct. Mater.*, 2012, **22**, 1578-1585.
- 23 Q. Jiwei, L. Yudong, Y. Ming, W. Qiang, C. Zongqiang, P. Jingyang, L. Yue, W. Wudeng, Y. Xuanyi, S. Qian and X. Jingjun, *Nanoscale Res. Lett.*, 2013, **8**, 495.
- 24 I. Tanahashi, *Bull. Chem. Soc. Jpn.*, 2007, **80**, 2019-2023.
- 25 I. Tanahashi and Y. Harada, *Nanoscale Res. Lett.*, 2014, **9**, 298.
- 26 H. Hada, Y. Yonezawa, A. Yoshida and A. Kurakake, *J. Phys. Chem.*, 1976, **80**, 2728- 2731.
- 27 P. Pinkhasova, L. Yang, Y. Zhang, S. Sukhishvili and H. Du, *Langmuir*, 2012, **28**, 2529-2535.
- 28 Y. Lu, G. L. Liu and L. P. Lee, *Nano Lett.*, 2005, **5**, 5-9.

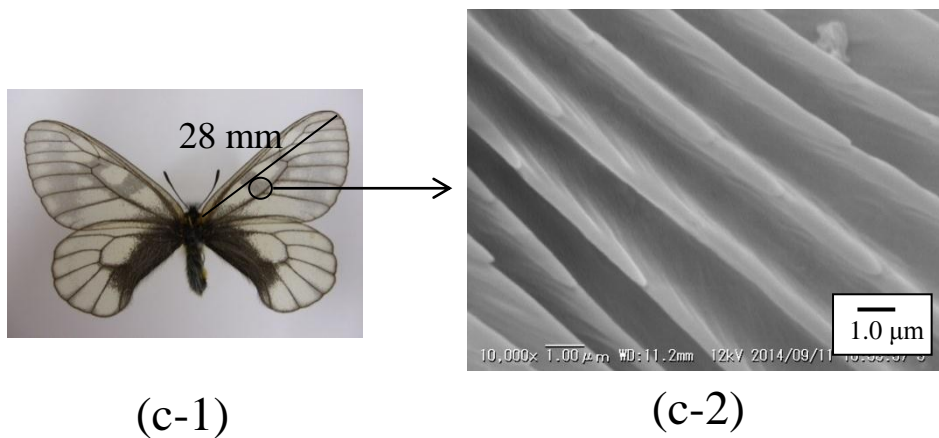
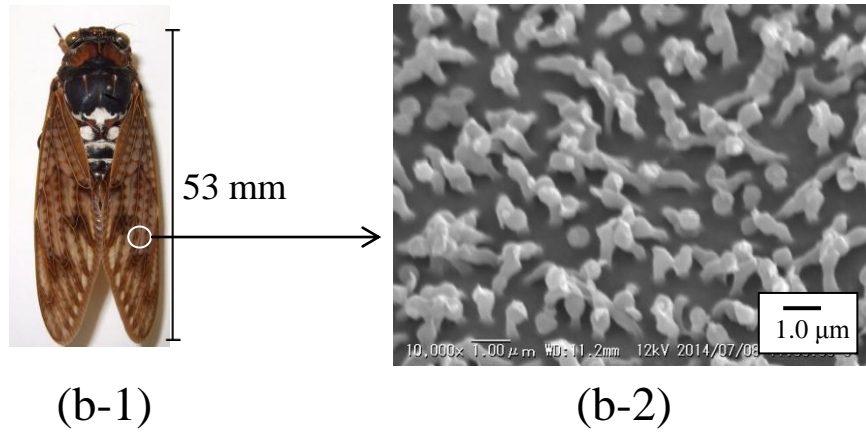
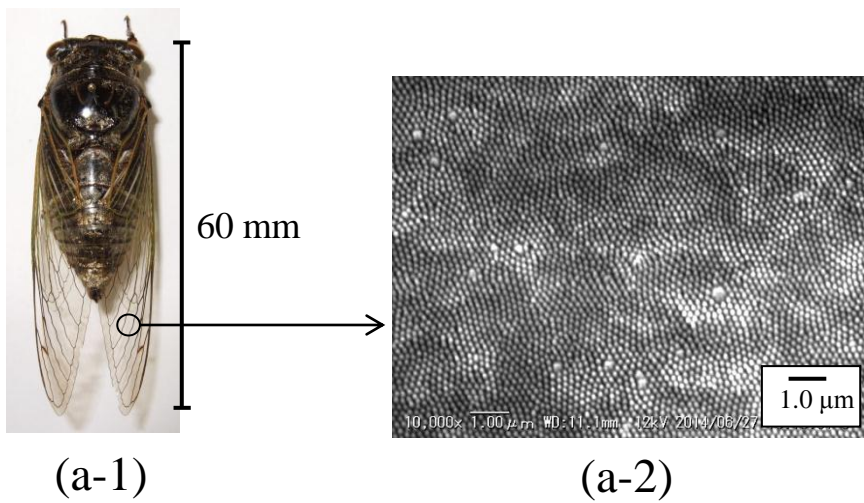
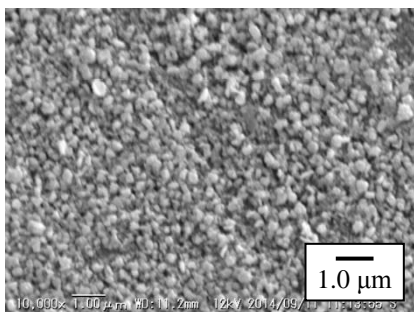
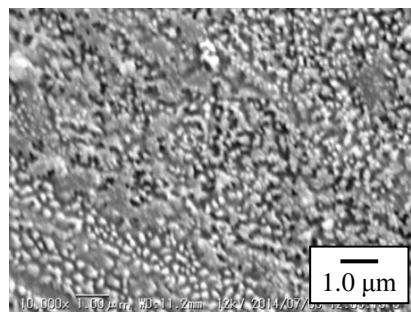


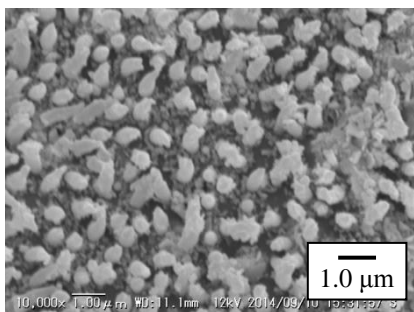
Figure 1
I. Tanahashi



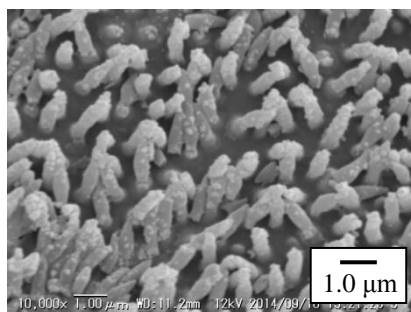
(a-3)



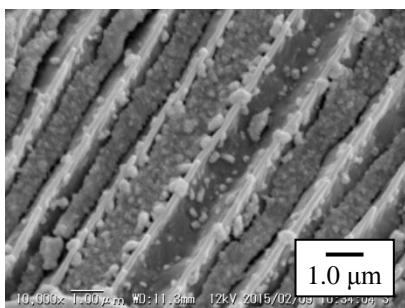
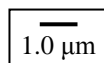
(a-4)



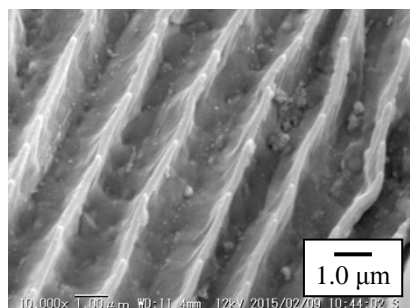
(b-3)



(b-4)



(c-3)



(c-4)

Figure 2
I. Tanahashi

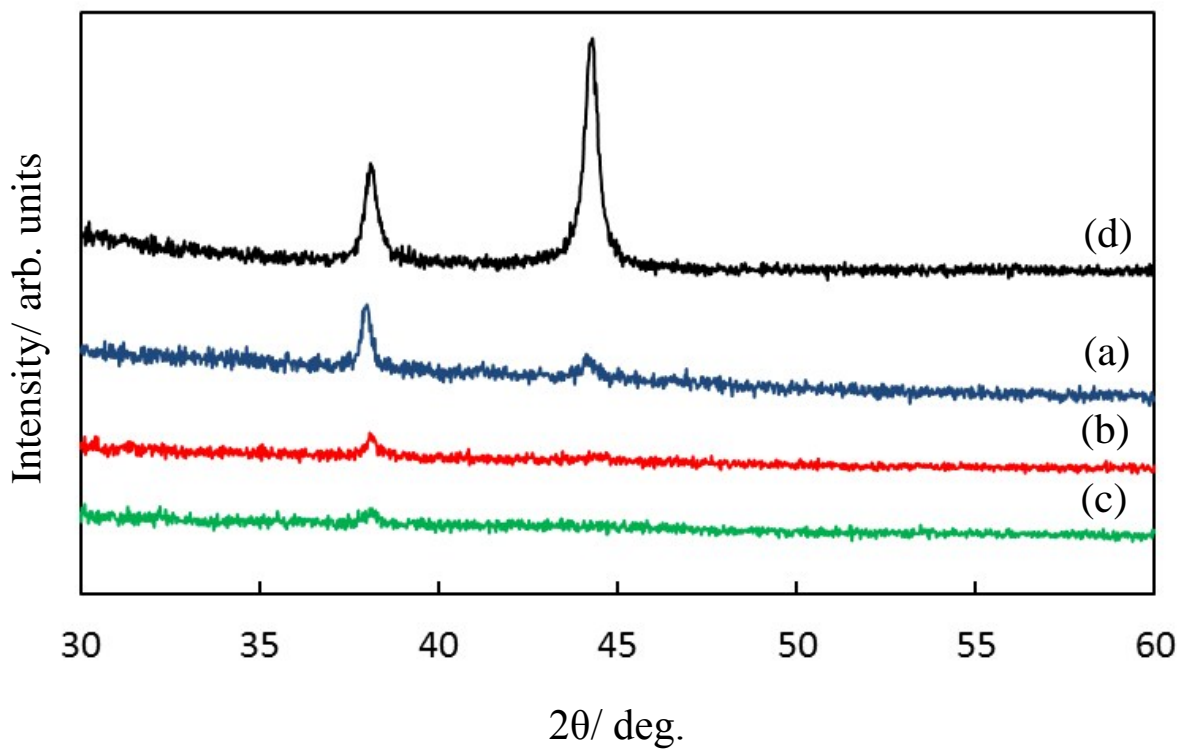


Figure 3
I. Tanahashi

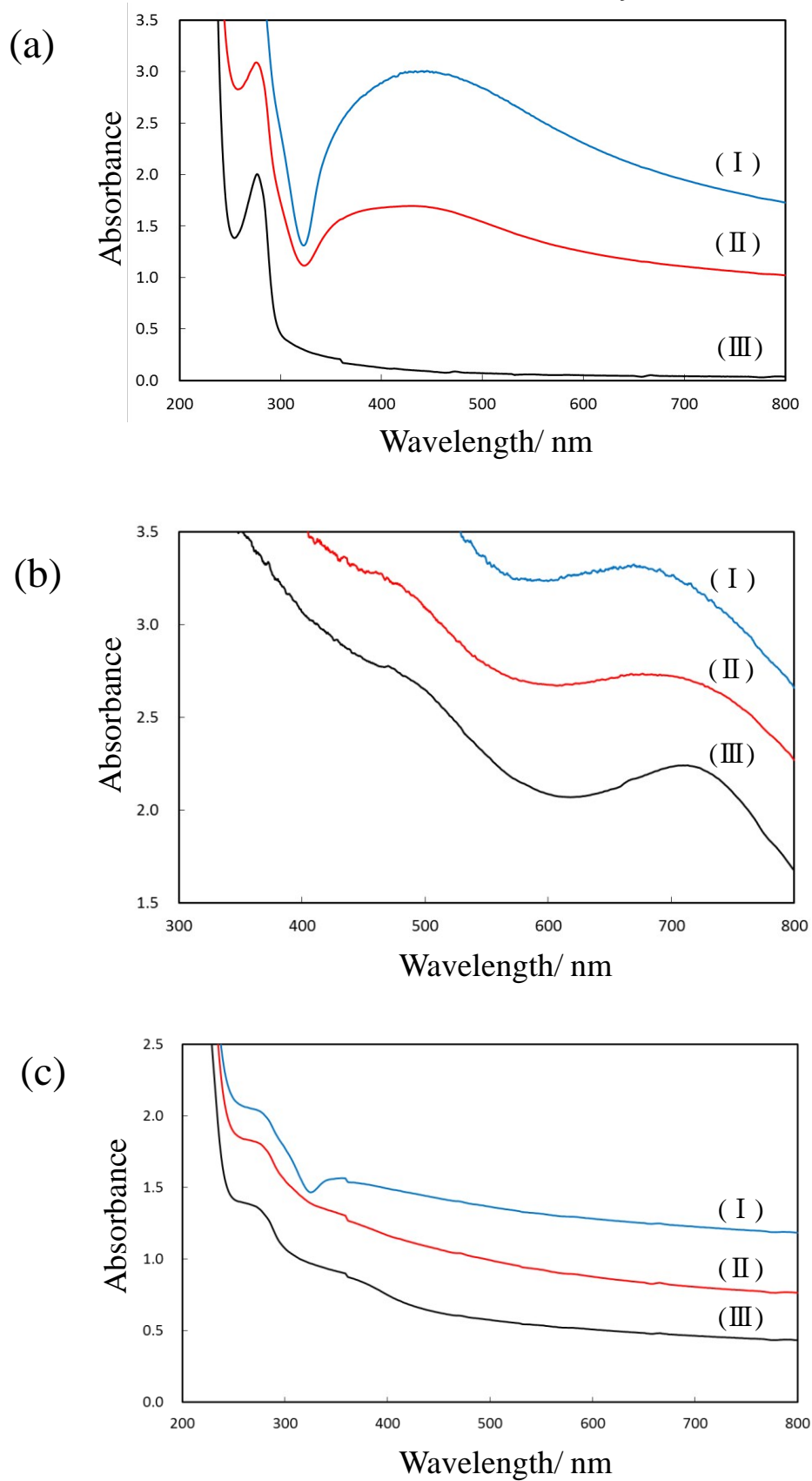


Figure 4
I. Tanahashi

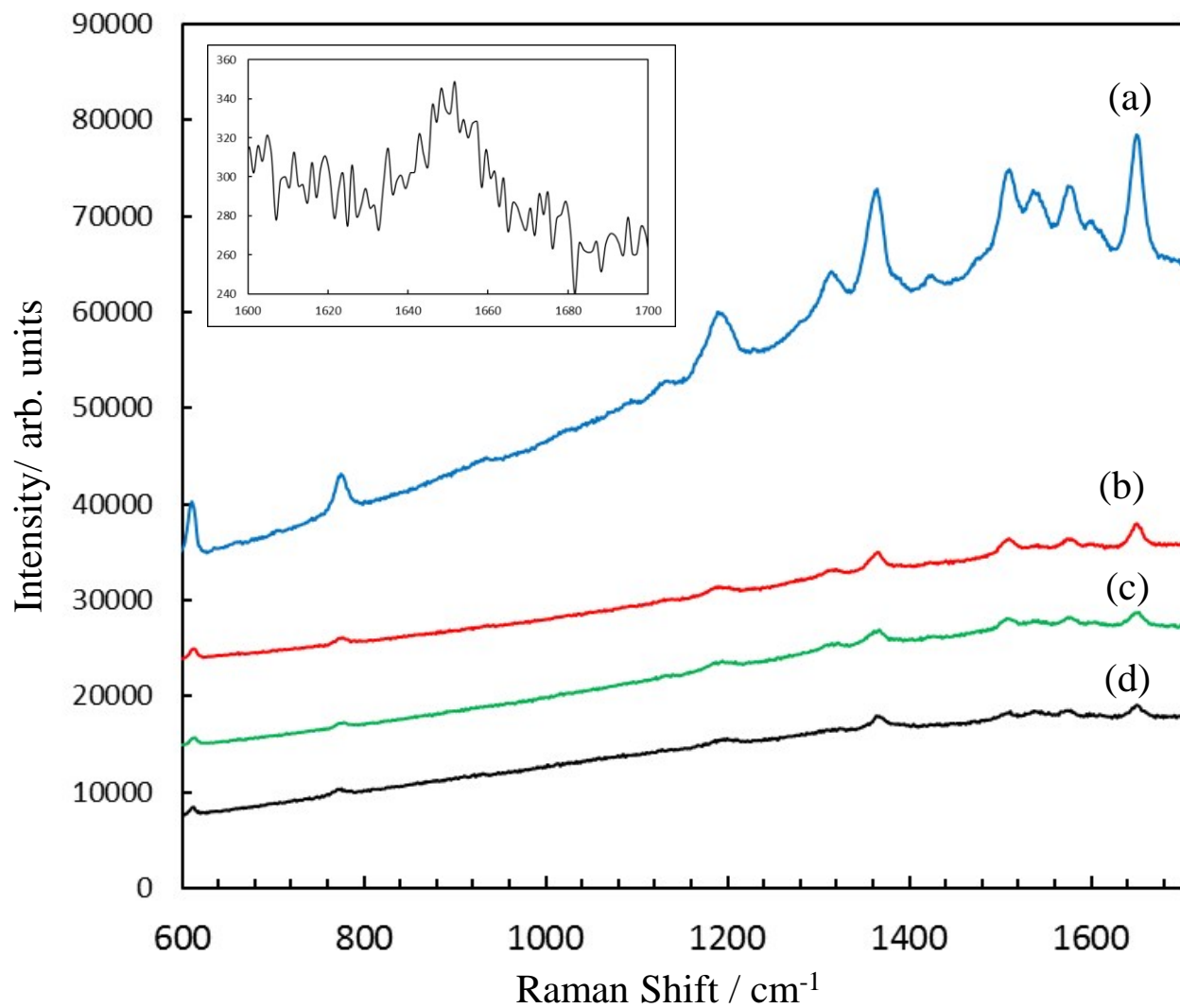


Figure 5
I. Tanahashi

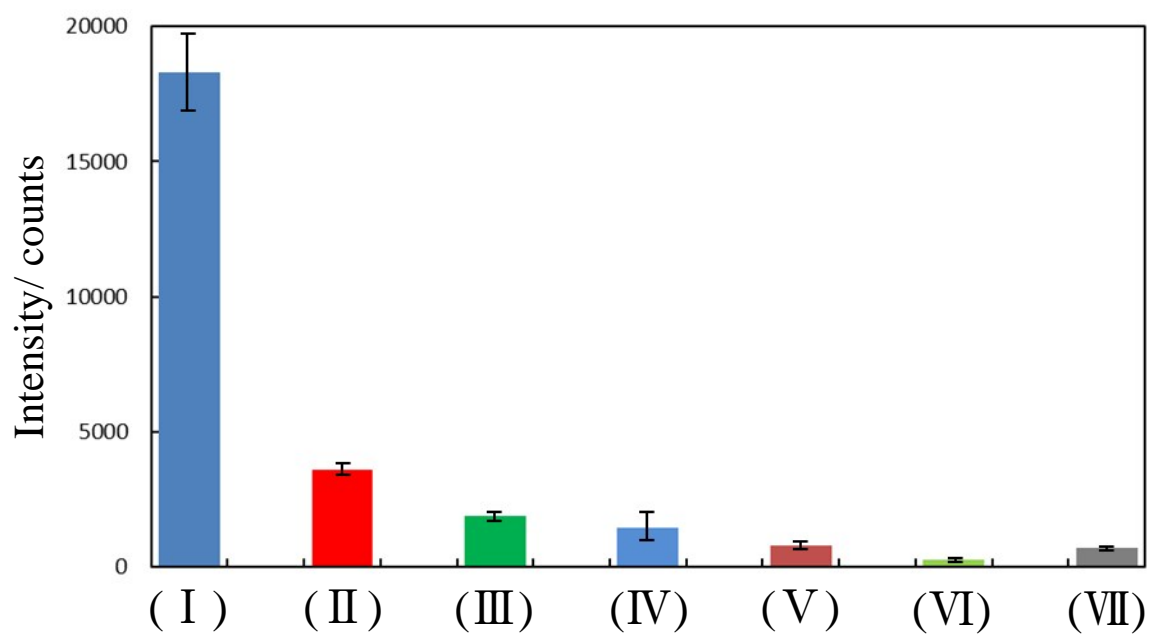


Figure 6
I. Tanahashi